



Synthesis, characterization and photocatalytic activity of crystalline Mn(II)Cr(III)-layered double hydroxide

Zita Timár^{a,b}, Gábor Varga^{a,b}, Szabolcs Muráth^{a,b}, Zoltán Kónya^{c,d}, Ákos Kukovecz^{c,e}, Viktor Havasi^e, Albert Oszkó^f, István Pálinkó^{a,b}, Pál Sipos^{b,g,*}

^a Department of Organic Chemistry, University of Szeged, Dóm tér 8, Szeged, H-6720, Hungary

^b Materials and Solution Structure Research Group, Institute of Chemistry, University of Szeged, Aradi Vértanúk tere 1, Szeged, H-6720, Hungary

^c Department of Applied and Environmental Chemistry, University of Szeged, Rerrich Béla tér 1, Szeged, H-6720, Hungary

^d MTA-SZTE Reaction Kinetics and Surface Chemistry Research Group, Rerrich Béla tér 1, Szeged, H-6720, Hungary

^e MTA-SZTE "Lendület" Porous Nanocomposites Research Group, Rerrich Béla tér 1, Szeged, H-6720, Hungary

^f Department of Physical Chemistry and Material Science, University of Szeged, Aradi Vértanúk tere 1, Szeged, H-6720, Hungary

^g Department of Inorganic and Analytical Chemistry, University of Szeged, Dóm tér 7, Szeged, H-6720, Hungary

ARTICLE INFO

Article history:

Received 6 July 2016

Received in revised form

30 November 2016

Accepted 16 December 2016

Available online 23 December 2016

Keywords:

Layered double hydroxide

Heterogeneous photocatalysis

Photodegradation of methylene blue

UV-vis light irradiation

ABSTRACT

Photocatalytic decomposition of methylene blue was attempted over as-prepared Mn(II)Cr(III)-layered double hydroxide (LDH) containing Mn(II) and Cr(III) in 2:1 molar ratio. The LDH was prepared by the co-precipitation method, and was found to form at pH = 10 and at 80 °C following 24 h hydrothermal treatment. The Mn₂Cr-LDH thus obtained was structurally characterized by X-ray diffractometry, scanning electron microscopy and energy-dispersive X-ray spectroscopy. The Mn₂Cr-LDH displayed significant photocatalytic activity in the degradation of methylene blue under illumination with UV-vis light. The photocatalytic performance of the phase-pure and uncalcined Mn₂Cr-LDH is practically identical to that of the commercially available Degussa P25 TiO₂, and it was found to remain unaltered over five consecutive photocatalytic runs. The presence of the LDH structure in the composite is the prerequisite of the photocatalytic activity. Applying increasing calcination temperature, the LDH structure gradually collapses, and the Mn₂Cr-LDH transforms to photocatalytically inactive double oxide.

© 2016 Elsevier B.V. All rights reserved.

1. Introduction

The use of heterogeneous photocatalysis in various industrial processes steadily increases, and photocatalysts are in the process of becoming more and more popular in a variety of practical applications. Even though traditional (non-photoactive) catalysts are still predominate and are produced in much higher amounts, photocatalysts offer a viable and environmentally friendly alternative in, e.g., cleaning industrial sewage [1,2].

Certain types of composite materials are capable of catalysing transformations of both organic and inorganic compounds in a photocatalytic way [3]. Layered double hydroxides (LDHs) were among those tested. At the early stage of these studies, it was shown that both the treatment of the composite compound before the reaction and the reaction conditions play crucial role in the pho-

tocatalytic efficiency [4,5]. Transition metal-containing LDHs are usually poorly crystalline materials [6,7], and as long as this is the case, photocatalysts of poor performance was possible to be prepared of them. On the other hand, with increasing crystallinity, the specific surface area of the photocatalyst inevitably decreases, which may also exert an adverse effect on the photoactivity [8,9].

In this work, our aims were (i) the synthesis of manganese-chromium containing LDH samples with optimal crystallinity and (ii) their use as photocatalysts in the degradation of methylene blue, as model compound.

The trivalent cation of choice was Cr(III), because of its expected photoactivity [10]. It has been already shown that ZnCr-LDHs, due to the presence of Cr(III), displays photocatalytic activity [10], which can be enhanced by doping it with Tb(III) [11] or including graphene in the composite [12]. Although the divalent cationic partner is most often Zn(II) in the layers, some examples for applying Cu(II), Ni(II) and even Mg(II) are known [10,13,14]. It is to be noted, however, that Cr(III)-containing LDHs were only seldom made [15,16] and details about the synthesis is even more scarcely

* Corresponding author at: Department of Inorganic and Analytical Chemistry, University of Szeged, Dóm tér 7, Szeged, H-6720 Hungary.

E-mail address: sipos@chem.u-szeged.hu (P. Sipos).

communicated [16]. The reason is probably the difficulty in preparing phase-pure material [15].

Methylene blue is a cationic dye easily adsorbed over various materials like titanate nanowires [17], titanate nanotubes [18,19]. It was our choice in testing the photocatalytic activity of our MnCr-LDH preparation, since it proved to be useful substance in probing the photocatalytic properties of various LDH composite materials [20,21], recently.

2. Experimental

For obtaining sufficiently crystalline LDH, the synthesis parameters were necessary to be optimized first. The pH and the temperature used during the synthesis of the LDHs and the molar ratio of the two metal ions were suspected to be critical factors in terms of the efficiency of the photocatalyst prepared, but other processing parameters like those of the hydrothermal treatment are also known to greatly influence crystallization and photocatalytic efficiency. Accordingly, the following experimental parameters were systematically varied during the preparation: pH (from 8 to 11); the preparation temperature (from 25 to 80 °C), the ratio between the di- and the trivalent ions (from 2:1 to 4:1).¹ Both nitrate and chloride salts were used for the syntheses; however, chloride salts were omitted, as it was observed that the LDH did not precipitate from the reaction mixture if chloride salts were utilized. During a typical, e.g., Mn₂Cr-LDH, synthesis *via* co-precipitation, a mixture of analytical grade Mn(NO₃)₂ × 4H₂O (30 mmol) and Cr(NO₃)₃ × 9H₂O (15 mmol) (both are Reanal products) was dissolved in 100 mL of distilled water, and was stirred at pH = 10 for 24 h. The pH was adjusted *via* adding a solution of 3 M NaOH to the system, the pH of which was monitored with a calibrated glass electrode. The suspension was filtered, washed with distilled water and the blackish-blue crystals were dried for 24 h *in vacuo* over P₂O₅. Hydrothermal treatment [22] was carried out in a closed Pyrex glass vessel at 80 ± 3 °C, using continuous stirring. The resulting suspension was filtered and dried for 24 h *in vacuo* over P₂O₅.

The materials prepared were characterized by various methods.

X-ray diffractometry (XRD) was used to verify the success (or the failure) of the preparation of the LDHs, since LDHs are known to have characteristic XRD patterns. The XRD traces of the various samples were recorded on a Rigaku XRD-6000 diffractometer, using CuK_α radiation (λ = 0.15418 nm) at 40 kV, 30 mA.

Scanning electron microscopy (SEM) was also employed to make the characteristic hexagonal morphology of the LDHs visible. The morphology of thin films was investigated using a Hitachi S-4700 scanning electron microscope with the accelerating voltage of 10–18 kV.

Energy dispersive X-ray (EDX) microspectroscopy gives a (semi)quantitative picture of the components in the material synthesized. EDX data were obtained on a Röntec QX2 energy dispersive microanalytical system from two different parts of the sample. The system was coupled to the SEM, and provided with the elemental map of the chosen region of the sample.

To identify interlayer anions, IR spectra of some selected samples were recorded. For this, a BIO-RAD Digilab Division FTS-65A/896 FT-IR spectrophotometer with 4 cm⁻¹ resolution, using DRS technique was employed. Spectra in the 4000–600 cm⁻¹ wavenumber range were recorded, but the most relevant 1850–600 cm⁻¹ range will be displayed and discussed. 256 scans were collected for each spectrum.

The band gap of the material prepared was determined from the UV–vis spectrum registered on Ocean Optics USB4000 spectrome-

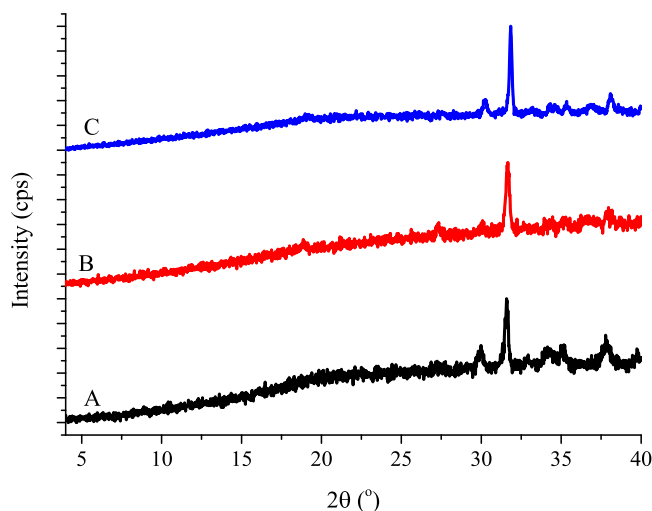


Fig. 1. XRD patterns for the solid substances obtained from a solution containing Mn(II) and Cr(III) in a molar ratio of 2:1 at various pH-s: A: pH=9, B: pH=10, C: pH=11; the temperature of the reaction mixture was T = 25 °C.

ter with a DH-2000-BAL UV–vis-NIR light source measuring diffuse reflectance mode and using BaSO₄ as reference. The spectrum was analyzed with the SpectraSuite package. The band-gap energy was determined from the extrapolation of the straight section of the modified Kubelka-Munk function plotted vs. energy of the incident light. Bandgap determination was done only for the phase pure LDH, as this specimen was exclusively used for the photocatalytic tests.

For the photocatalytic tests, 1 mg of catalyst in 200 mL solution was used, the pH was controlled by a buffer based on KH₂PO₄ (0.15 M). To determine the best parameter set for the photocatalytic degradation, the pH of the solution (7–10), the temperature of the reaction mixture (8–50 °C) and the concentration of substrate, methylene blue that is (product of Aldrich Chemicals) were systematically varied. The photoreactor was an open Pyrex glass vessel. An OSRAM Power Star HCL-TC 70 W/WDL lamp (λ = 360–800 nm) was applied at a fixed position for irradiating the reactor; the irradiation took place from vertical position, ca. 10 cm from the inlet of the vessel. The degradation of the dye was followed by UV–vis spectrometry on a Shimadzu UV-1650 spectrophotometer. Absorbance values at absorption maximum of methylene blue (665 nm) were recorded.

The X-ray photoelectron spectra (XPS) of the freshly prepared and the used samples were taken with a SPECS instrument equipped with a PHOIBOS 150 MCD 9 hemispherical electron energy analyzer (Germany) operated in the FAT mode. The excitation source was the K_α radiation of magnesium (hν = 1253.6 eV) and aluminum (hν = 1486.3 eV) anodes. The X-ray gun was operated at 180 W power (12 kV, 15 mA). The pass energy was set to 20 eV, the step size was 25 meV, and the collection time in one channel was 150 ms.

3. Results and discussion

3.1. Preparation and structural characteristics of the Mn₂Cr-LDH samples

During the preparative work, first, the synthesis of Mn_nCr-LDH with appreciable crystallinity was aimed at. As simple co-precipitation without hydrothermal post-treatment is reported to be a very efficient way of LDH preparation in general, therefore, this trivial synthesis route was initially employed [22,23]. As it is shown in Figs. 1–3, *via* using this preparation method, the

¹ In the acronym used for the LDHs prepared, *i.e.*, Mn_nCr, n stands for the Mn:Cr molar ratio in the solid.

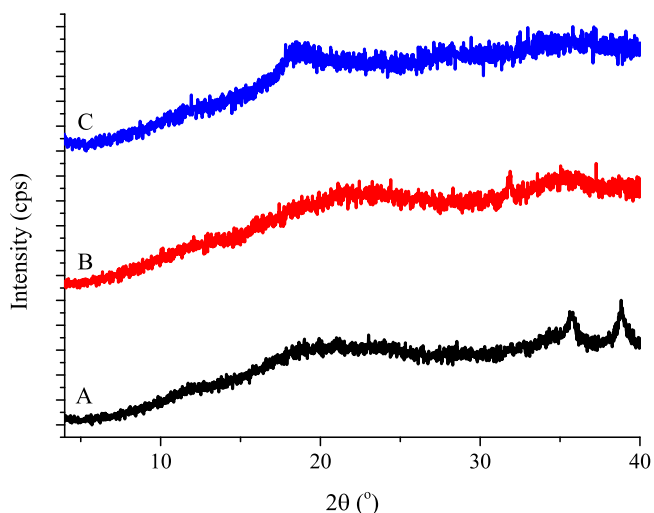


Fig. 2. XRD patterns for the solid substances obtained from a solution containing Mn(II) and Cr(III) at various molar ratios: A: 2:1; B: 3:1; C: 4:1. The syntheses were performed at pH = 10 and T = 25 °C throughout.

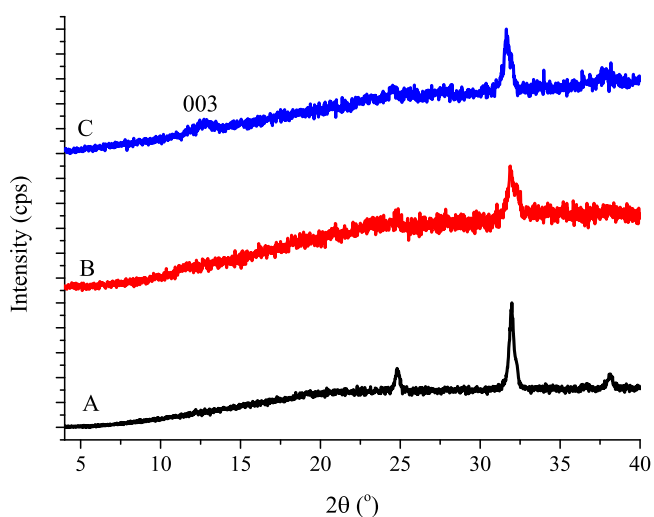


Fig. 3. XRD patterns for the solid obtained from a solution containing Mn(II) and Cr(III) in a molar ratio of 2:1 at various temperatures: A: T = 40 °C, B: T = 60 °C, C: T = 80 °C. The pH of the reaction mixture was 10 throughout. The weak feature at $2\theta \approx 12^\circ$ denoted by (003) is likely to be a reflection stemming from some Mn_2Cr -LDH.

desired LDH formation could not be observed either *via* systematically changing the pH (Fig. 1), the reactant ratio (Fig. 2) or the temperature (Fig. 3). The lack of the characteristic (003) reflection of the LDHs around $2\theta \approx 12^\circ$ (except for the weak feature corresponding to in Fig. 3C, see below) unambiguously prove, that the use of these (otherwise commonly employed) synthesis parameters did not lead to pure and highly crystalline Mn_nCr -LDH.

In Fig. 3C, under superambient conditions (T = 80 °C), the formation of some Mn_2Cr -LDH could be observed. Accordingly, it was hypothesised, that a longer hydrothermal treatment may lead to the formation of the desired Mn_2Cr -LDH. Upon using hydrothermal treatment at 80 °C for 24 h, the appearance of the XRD patterns characteristic to the LDH (Fig. 4) could be observed. From this, it can also be stated that the by-products also disappeared, and the basal spacing was calculated as $d = 0.744$ nm (with estimated a [14,24] and calculated c lattice parameters of 4.7 nm and 2.23 nm, respectively [24]). On the basis of the XRD patterns, the sample obtained could be considered as phase pure. The XRD pattern and the BET surface area (56.4 m²/g) of the successfully prepared sample did

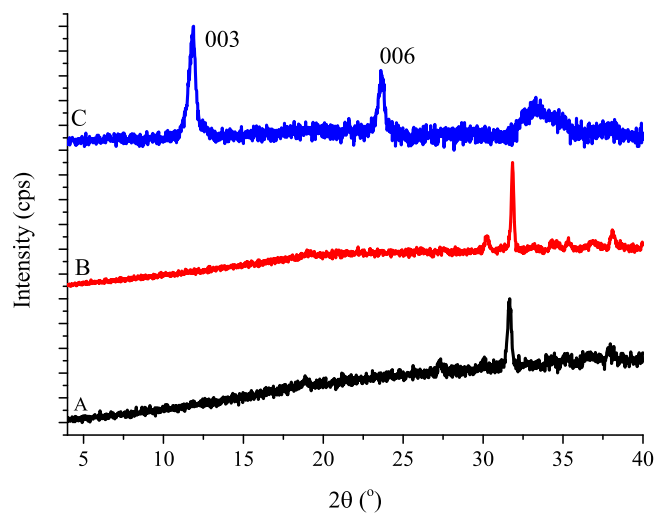


Fig. 4. XRD patterns for the solid substances obtained from a solution containing Mn(II) and Cr(III) in a molar ratio of 2:1, subjected to hydrothermal treatment for 24 h at various temperatures: A: T = 40 °C, B: T = 60 °C, C: T = 80 °C. The pH of the reaction mixture was 10 throughout.

not change within two months from the synthesis indicating considerably stability. The average thickness of the LDH particles were calculated from the Debye-Scherrer equation and was found to be 3.1 nm.

For the phase-pure Mn_2Cr -LDH specimen, the XRD pattern of which is shown in Fig. 4C, the SEM images were also recorded. From the pictures, the laminar hexagonally-shaped morphology, typical of LDHs can be observed (Fig. 5).

The SEM-EDX elemental map obtained for the phase-pure Mn_2Cr -LDH sample is displayed in Fig. 6. It shows that both the manganese and chromium are evenly distributed.

The IR spectrum of the phase-pure Mn_2Cr -LDH (Fig. 7) shows the characteristic vibration of the intercalated NO_3^- ion at 1405 cm⁻¹ [25]. As the IR band of the carbonate ion appears very close to that of nitrate, some contribution from possible carbonate contamination may also be present in this signal. The other two distinct vibration bands correspond to the LDH structure, and are associated with β -OH (1630 cm⁻¹) [26] and Cr–O (780 cm⁻¹) modes [25].

DRS spectrum of the as-prepared phase pure Mn_2Cr -LDH was also recorded (Fig. 8). Assuming direct band gap transition and extrapolating the straight section of the modified Kubelka-Munk function plotted vs. energy of the incident light resulted in band gap energy of 1.46 eV. This corresponds to 850 nm wavelength, which is consistent with the blackish-blue colour of the specimen. Taking indirect band gap transition, its energy was not possible to be accurately computed (being at ca. 0.8 eV and therefore falling outside the measurement range of the instrument). Comparing the two types of band gap energies, direct band gap transition seems to be more realistic for the phase pure Mn_2Cr -LDH semiconductor.

3.2. Photocatalysis of methylene blue over Mn_2Cr -LDH

The photocatalytic activity of the phase-pure Mn_2Cr -LDH composite was tested in the photodegradation of methylene blue (MB) under UV–vis light irradiation. In the absence of the catalyst, it was observed that the decomposition of MB was negligible even after an extended period of time. It was reported previously by others that upon UV–vis irradiation, more than 10% of the MB decomposed within 6 h; however, those reactions were performed under acidic conditions [27]. At the beginning of the catalytic experiments, MB was allowed to adsorb over the surface of the catalysts; in each case, one hour “dark time” was allowed, before switching the illu-

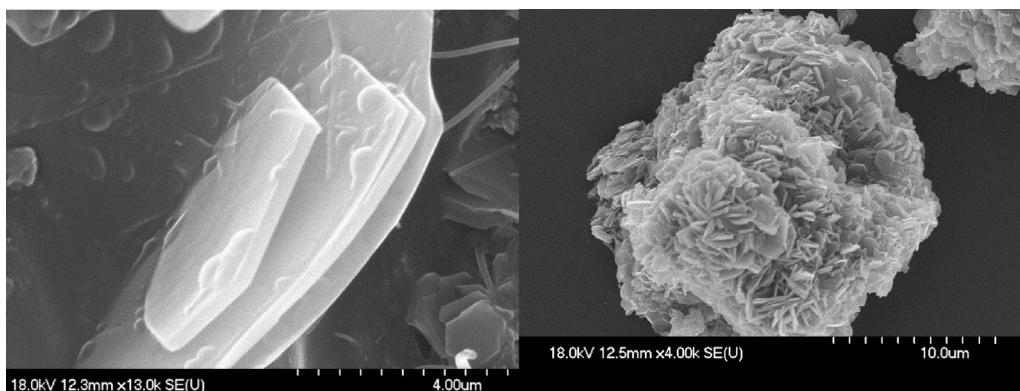


Fig. 5. SEM images for $\text{Mn}_2\text{Cr-LDH}$ (hydrothermally treated at $T=80^\circ\text{C}$ for 24 h at $\text{pH}=10$).

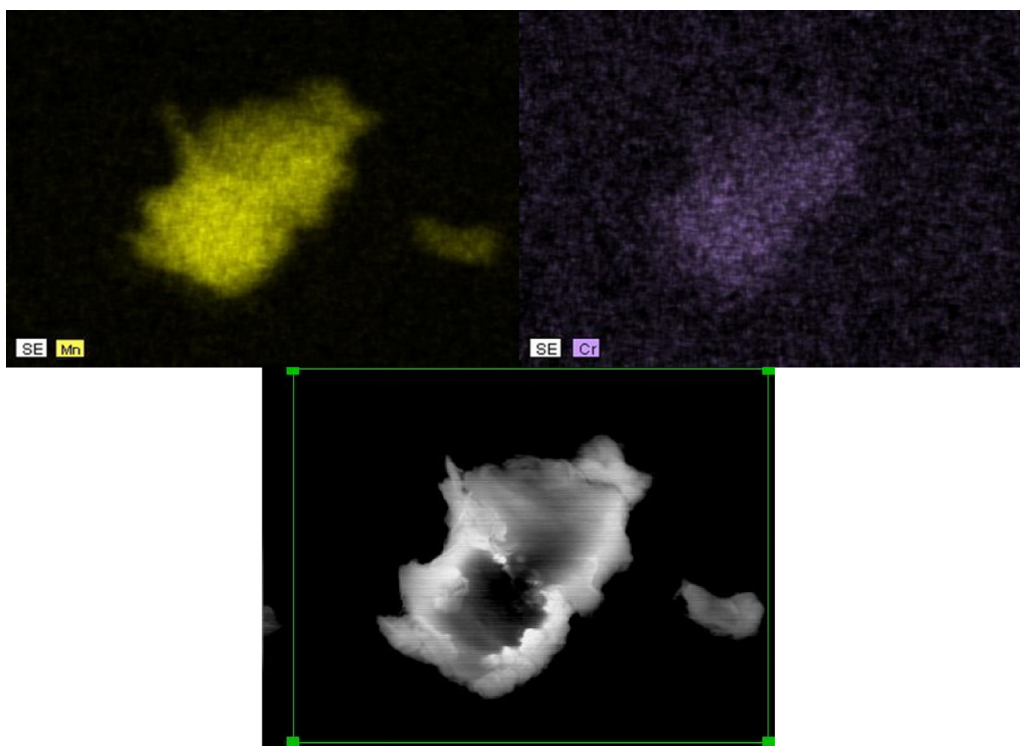


Fig. 6. SEM–EDX elemental maps for the phase-pure $\text{Mn}_2\text{Cr-LDH}$ (hydrothermally treated at $T=80^\circ\text{C}$ for 24 h at $\text{pH}=10$).

mination on. The initial decrease of the MB concentration *prior* to switching on the light source is most probably associated with this surface absorption of the substrate.

3.2.1. The effect of pH during the reaction

The most important parameter that affect degradation was found to be the pH of the solution (Fig. 9). It was found that the photoreaction commenced with an induction period at each pH, and was the faster, when the pH of the solution was adjusted to 9. Under these conditions, the degradation of the MB reached >80% after 120 min. At higher and at lower pH, the reaction rate was significantly lower. At $\text{pH}=7$, apparently the c/c_0 vs. time curve starts increasing after ca. 60 min (Fig. 9A), most probably, due to the formation of some intermediate, which also absorbs the light at the detection wavelength. These observations strongly suggest that the mechanism of the photodegradation of MB over $\text{Mn}_2\text{Cr-LDH}$ composite is strongly pH-dependent [28].

3.2.2. Effect of MB concentration

The initial concentration of the MB can be an important factor in the photodegradation reaction. Therefore, in further experiments, its concentration was systematically changed from 20 mg/L to 40 mg/L. Fig. 10 attests that the degree of degradation varied in the 70–92% range. Taking into consideration the errors in these photocatalytic test measurements, it seems reasonable to suggest, that in the MB concentration range covered, the reaction rate is roughly independent of the substrate concentration. In the subsequent measurements, $c_0 = 30$ mg/L substrate concentration was employed.

3.2.3. Effect of photocatalyst calcination

During the subsequent experiments, the phase-pure $\text{Mn}_2\text{Cr-LDH}$ composite was subjected to annealing at various temperatures (250, 500 and 750°C) for 24 h. Following this calcination procedure, the photodegradation experiments were repeated using the optimized decomposition conditions ($c_0 = 30$ mg/L, $\text{pH}=9$, $T=25^\circ\text{C}$). The effect of the various calcination temperatures on the photo-

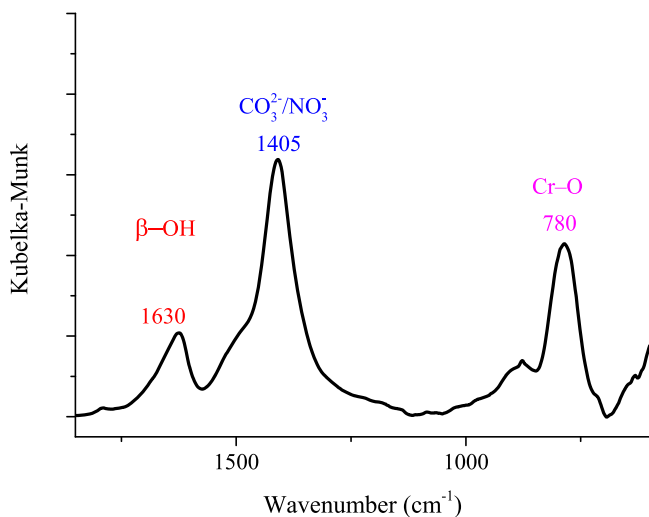


Fig. 7. IR spectrum of phase-pure $\text{Mn}_2\text{Cr-LDH}$.

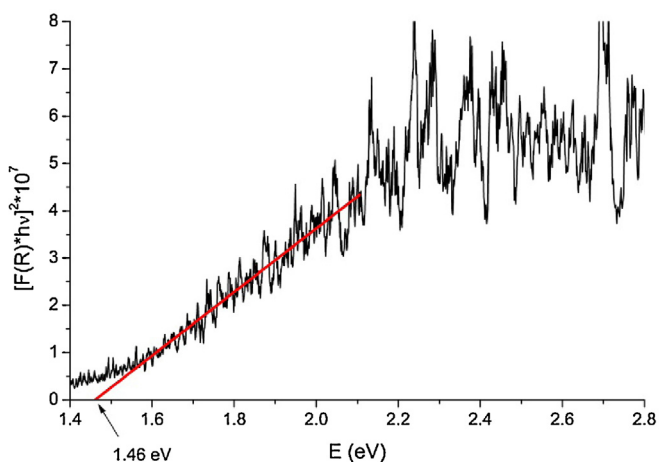


Fig. 8. Tauc plot of the phase pure $\text{Mn}_2\text{Cr-LDH}$.

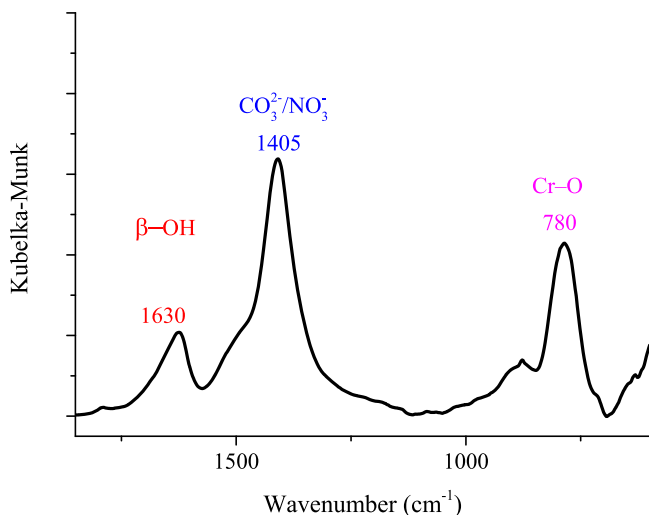


Fig. 9. The photodegradation of MB expressed as c/c_0 as a function of illumination time over phase-pure $\text{Mn}_2\text{Cr-LDH}$ composite at various pH values and at 25 °C. A: pH = 7, B: pH = 9, C: pH = 10 (initial concentration of MB: $c_0 = 30 \text{ mg/L}$).

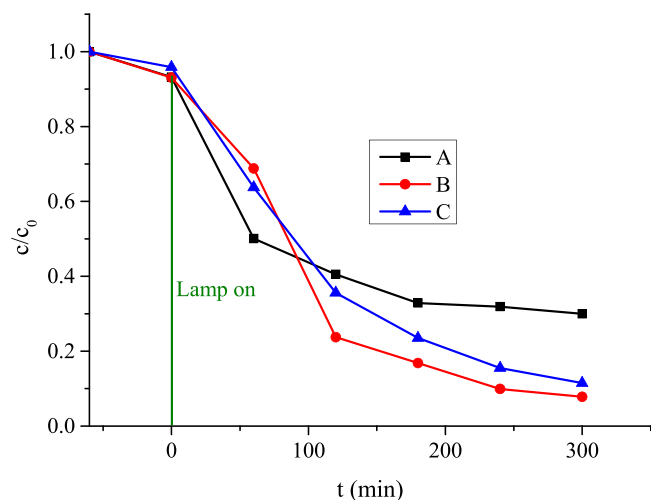


Fig. 10. The photodegradation of MB expressed as c/c_0 as a function of illumination time over phase-pure $\text{Mn}_2\text{Cr-LDH}$ composite at various initial concentration of MB. A: 20 mg/L; B: 30 mg/L; C: 40 mg/L pH = 9, $T = 25^\circ\text{C}$.

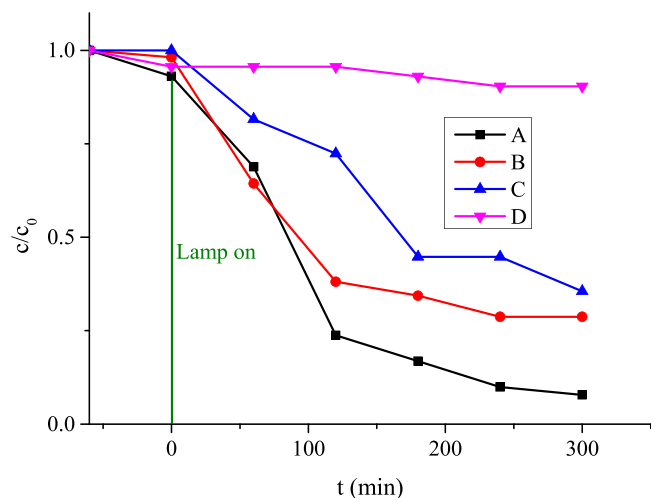


Fig. 11. The photodegradation of MB expressed as c/c_0 as a function of illumination time over phase-pure $\text{Mn}_2\text{Cr-LDH}$ composite calcined at various temperatures for 24 h. Calcination temperatures: A: no calcination; B: 250 °C; C: 500 °C; D: 750 °C. Conditions of photodegradation: $c_0 = 30 \text{ mg/L}$; pH = 9, $T = 25^\circ\text{C}$.

catalytic activity are displayed in Fig. 11, while the XRD patterns of the calcined phase-pure $\text{Mn}_2\text{Cr-LDH}$ composite is shown in Fig. 12.

It was observed that among the $\text{Mn}_2\text{Cr-LDH}$ samples, the uncalcined photocatalyst exhibited the highest photocatalytic activity. Increasing the calcination temperature resulted in a drastic and systematic decrease in the photocatalytic activity. Calcination at 750 °C for 24 h resulted in a material, which had practically no photocatalytic activity whatsoever. From Fig. 12, it is apparent that the increasing calcination temperature resulted in a gradual collapse of the LDH structure, and (most probably) resulted in the progressive formation of some sort of double oxide. Latter composite has no photocatalytic activity, as opposed to the composite having the layered structure. The photocatalytic activity of the various $\text{Mn}_2\text{Cr-LDH}$ samples clearly correlate with the proportion of the layered structure remaining after calcination. This observation strongly suggests that the presence of the ordered layered structure is advantageous for the photocatalytic activity of these composites in MB degradation; the highly regular structure helps in preserving the oxidation state of the cationic components of the as-prepared LDH.

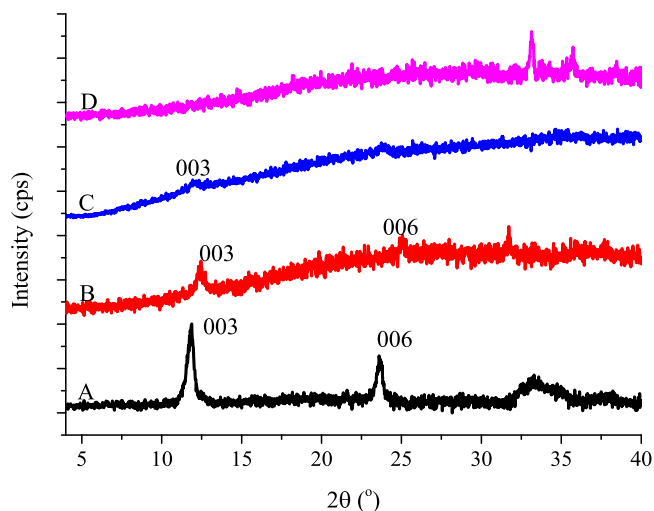


Fig. 12. XRD patterns of phase-pure $\text{Mn}_2\text{Cr-LDH}$ samples calcined at various temperatures for 24 h. Calcination temperatures: A: uncalcined sample, B: 250 °C, C: 500 °C, D: 750 °C.

To compare the performance of our best $\text{Mn}_2\text{Cr-LDH}$ sample with that of the commercially available Degussa P25 TiO_2 , MB photodegradation experiments were performed (Fig. 13) under identical conditions employing 1 mg photocatalyst of both solids in 200 cm^3 test solution. From this graph, it is apparent that the photocatalytic performance of the $\text{Mn}_2\text{Cr-LDH}$ composite was almost the same as that of P25.

The stability of the $\text{Mn}_2\text{Cr-LDH}$ photocatalyst was tested by reusing the samples five times in the MB degradation experiment, employing the optimal degradation conditions. After each run, the photocatalyst was removed *via* filtration and dried over P_2O_5 *in vacuo*, in the usual way. As shown in Fig. 14, the degradation efficiency did not change significantly after five cycles, suggesting that the photocatalyst prepared by us is reasonably stable and resistant to photocorrosion.

3.2.4. The XPS analysis of the as-prepared and the used catalyst

The oxidation of the cationic components of the LDH was studied with X-ray photoelectron spectroscopy before and after the reaction (Fig. 15). The photoelectron spectra revealed that the oxidation state of neither cationic component changed during the catalytic reaction.

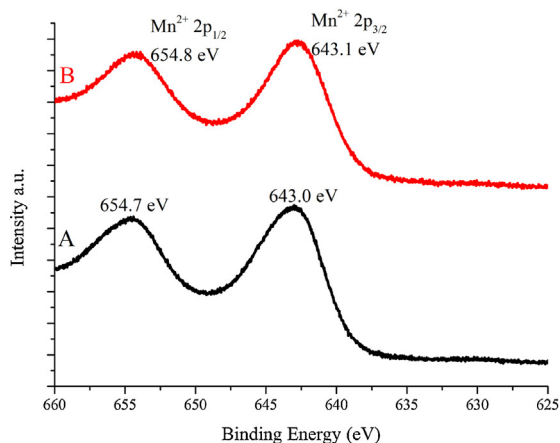


Fig. 15. The X-ray photoelectron spectra of the $\text{Mn}_2\text{Cr-LDH}$ catalyst as-prepared (A) and used (B).

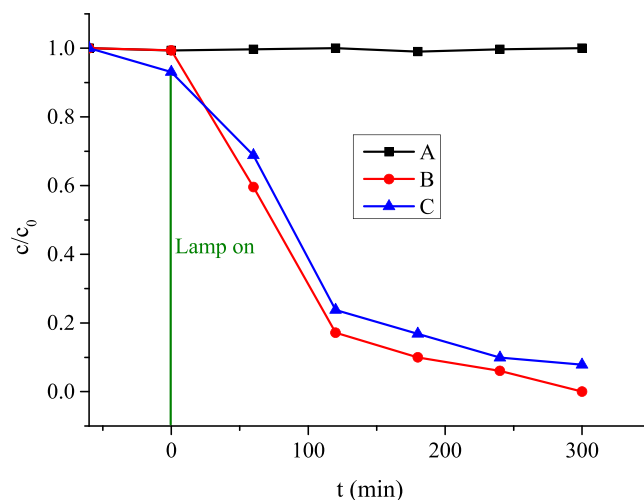


Fig. 13. The photodegradation of MB expressed as c/c_0 as a function of illumination time. A: No photocatalyst added; B: over Degussa P25 TiO_2 ; C: over phase-pure, uncalcined $\text{Mn}_2\text{Cr-LDH}$ composite. Conditions of photodegradation: $c_0 = 30 \text{ mg/L}$; $\text{pH} = 9$, $T = 25^\circ\text{C}$.

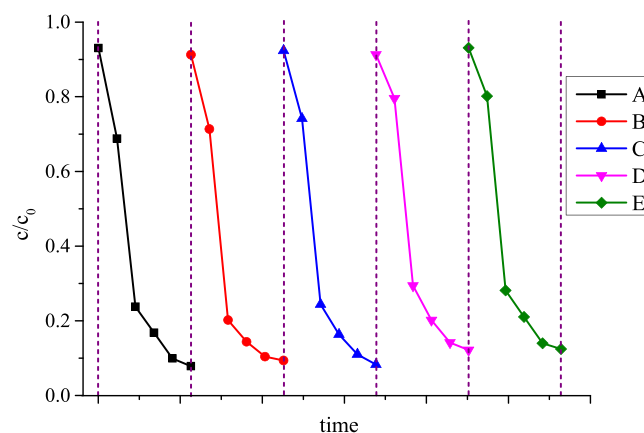


Fig. 14. The photodegradation of MB expressed as c/c_0 as a function of illumination time over five consecutive runs, denoted by A, B, C, D and E. Conditions of photodegradation: $c_0 = 30 \text{ mg/L}$; $\text{pH} = 9$, $T = 25^\circ\text{C}$.

4. Conclusions

In search for a layered double hydroxide that has appreciable heterogeneous photocatalytic activity, first the synthesis of crys-

talline Mn₂Cr-LDH was attempted. Phase-pure LDH was isolated from solutions containing the Mn(II) and Cr(III) in a 2:1 molar ratio and at pH = 10. For the formation of phase-pure Mn₂Cr-LDH, hydrothermal treatment at 80 °C for 24 h was found to be necessary; this way a Mn₂Cr-LDH sample with reasonable crystallinity was obtained. This material proved to be an efficient photocatalyst in the degradation reaction of MB. It was found that optimal photocatalytic performance was obtained, when the pH of the solution was adjusted to 9, and when the photocatalyst was not subjected to any calcination before the degradation experiment. The phase-pure and uncalcined Mn₂Cr-LDH photocatalyst displayed photocatalytic performance that was found to be practically identical to that of the commercially Degussa P25 TiO₂.

Acknowledgment

This work was supported by the National Science Fund of Hungary through OTKA NKFI 106234 and GINOP-2.3.2-15-2016-00013 grants. The financial help is highly appreciated.

References

- [1] S. Sikarwar, R. Jain, *Water Air Soil Pollut.* 226 (2015) 277.
- [2] G. Karaca, Y. Tasdemir, *J. Environ. Sci. Health A Tox. Hazard Subst. Environ. Eng.* 48 (2013) 855–861.
- [3] E. Dvininova, M. Ignat, P. Barvinschi, M.A. Smithers, E. Popovici, *J. Hazard. Mater.* 177 (2010) 150–158.
- [4] N. Ahmed, Y. Shibata, T. Taniguchi, Y. Izumi, *J. Catal.* 279 (2011) 123–135.
- [5] Y. Zhao, M. Wei, J. Lu, Z. Lin Wang, X. Duan, *ACS Nano* 3 (2009) 4009–4016.
- [6] M. del Arco, M.V.G. Galiano, V. Rives, R. Trujillano, P. Malet, *Inorg. Chem.* 35 (1996) 6362–6372.
- [7] H. Wan, J. Liu, Y. Ruan, L. Lv, L. Peng, X. Ji, L. Miao, J. Jiang, *ACS Appl. Mater. Interfaces* 7 (2015) 15840–15847.
- [8] M.F. de Almeida, C.R. Bellato, A.H. Mounteer, S.O. Ferreirac, J.L. Milagres, L.D.L. Miranda, *Appl. Surf. Sci.* 357 (2015) 1765–1775.
- [9] K. Abderrazek, F.S. Najoua, E. Srasra, *Appl. Clay. Sci.* 119 (2016) 229–235.
- [10] N. Baliarsingh, K.M. Parida, G.C. Pradhan, *Ind. Eng. Chem. Res.* 53 (2014) 3834–3841.
- [11] Y. Fu, F. Ning, S. Xu, H. An, M. Shao, M. Wei, *J. Mater. Chem. A* 4 (2016) 3907–3913.
- [12] J.L. Gunjajakar, I.Y. Kim, J.M. Lee, N.-S. Lee, S.-J. Hwang, *Energy Environ. Sci.* 6 (2013) 1008–1017.
- [13] A. de Roy, C. Forano, J.P. Besse, *Layered Double Hydroxides: Present and Future*, in: V. Rives (Ed.), Nova Science Publishers, Inc, New York, 2006, pp. 1–39 (Ch. 1).
- [14] J.W. Boclair, P.S. Braterman, J. Jiang, S. Lou, F. Yarberry, *Chem. Mater.* 11 (1999) 303–307.
- [15] V.R. Choudhary, D.K. Dumbre, B.S. Uphade, V.S. Narkhede, *J. Mol. Catal. A* 215 (2004) 129–135.
- [16] J.W. Boclair, P.S. Braterman, *Chem. Mater.* 11 (1999) 298–302.
- [17] E. Horváth, P.R. Ribič, F. Hashemi, L. Forró, A. Magrez, *J. Mater. Chem.* 22 (2012) 8778–8784.
- [18] L. Xiong, Y. Yang, J. Mai, W. Sun, C. Zhang, D. Wei, Q. Chen, J. Ni, *Chem. Eng. J.* 156 (2010) 313–320.
- [19] E. Horváth, I. Szilágyi, L. Forró, A. Magrez, *J. Coll. Interface Sci.* 416 (2014) 190–197.
- [20] S. Xia, L. Zhang, G. Pan, P. Qian, Z. Ni, *Phys. Chem. Chem. Phys.* 17 (2015) 5345–5351.
- [21] E.M. Seftel, M. Niarchos, Ch. Mitropoulos, M. Mertens, E.F. Vansant, P. Cool, *Catal. Today* 252 (2015) 120–127.
- [22] J.H. Choy, Y.M. Kwon, K.S. Han, S.W. Song, S.H. Chang, *Mater. Lett.* 34 (1998) 356–363.
- [23] F.M. Labajos, V. Rives, M.A. Ulibarri, *Mater. Sci.* 27 (1992) 1546–1552.
- [24] T.P.F. Teixeira, S.F. Aquino, S.I. Pereira, A. Dias, *Braz. J. Chem. Eng.* 31 (2014) 19–26.
- [25] F.A. Miller, C.H. Wilkins, *Anal. Chem.* 24 (1952) 1253–1294.
- [26] M. Mora, M.I. López, C. Jiménez-Sanchidrián, J.R. Ruiz, *Solid State Sci.* 13 (2011) 101–105.
- [27] Y. Zhou, L. Shuai, X. Jiang, F. Jiao, J. Yu, *Adv. Powder Technol.* 26 (2015) 439–447.
- [28] K. Abderrazek, F.S. Najoua, E. Srasra, *Appl. Clay. Sci.* 119 (2016) 229–235.